Divergent Mitochondrial Respiratory Chains in Phototrophic Relatives of Apicomplexan Parasites

Pavel Flegontov,[†,1,2] Jan Michálek,[†,1,3] Jan Janouškovec,[‡,4,5] De-Hua Lai,[§,1] Milan Jirků,[1,3] Eva Hajdušková,[1] Aleš Tomčala,[1] Thomas D. Otto,[6] Patrick J. Keeling,[4,5] Arnab Pain,[7] Miroslav Oborník,[*,1,3,8] and Julius Lukeš[*,1,3,5]

[1]Institute of Parasitology, Biology Centre, Czech Academy of Sciences, České Budějovice, Czech Republic

[2]Life Science Research Centre, Department of Biology and Ecology, Faculty of Science, University of Ostrava, Ostrava, Czech Republic

[3]Faculty of Science, University of South Bohemia, České Budějovice, Czech Republic

[4]Department of Botany, University of BC, Vancouver, Canada

[5]Canadian Institute for Advanced Research, Toronto, ON, Canada

[6]Wellcome Trust Sanger Institute, Hinxton, United Kingdom

[7]Biological and Environmental Sciences and Engineering Division, King Abdullah University of Science and Technology, Thuwal, Kingdom of Saudi Arabia

[8]Institute of Microbiology, Czech Academy of Sciences, Třeboň, Czech Republic

[†]These authors contributed equally to this work.

[‡]Present address: San Diego State University, San Diego, CA

[§]Present address: Center for Parasitic Organisms, School of Life Sciences, Sun Yat-Sen University, Guangzhou, People's Republic of China

***Corresponding author:** E-mail: obornik@paru.cas.cz; jula@paru.cas.cz.

Associate editor: David Irwin

Abstract

Four respiratory complexes and ATP-synthase represent central functional units in mitochondria. In some mitochondria and derived anaerobic organelles, a few or all of these respiratory complexes have been lost during evolution. We show that the respiratory chain of *Chromera velia*, a phototrophic relative of parasitic apicomplexans, lacks complexes I and III, making it a uniquely reduced aerobic mitochondrion. In *Chromera*, putative lactate:cytochrome *c* oxidoreductases are predicted to transfer electrons from lactate to cytochrome *c*, rendering complex III unnecessary. The mitochondrial genome of *Chromera* has the smallest known protein-coding capacity of all mitochondria, encoding just *cox1* and *cox3* on heterogeneous linear molecules. In contrast, another photosynthetic relative of apicomplexans, *Vitrella brassicaformis*, retains the same set of genes as apicomplexans and dinoflagellates (*cox1*, *cox3*, and *cob*).

Key words: **respiratory chain, Apicomplexa, Chromera, anaerobic metabolism, evolution, Vitrella.**

Introduction

Although all extant mitochondria are believed to originate from a single endosymbiotic event, mitochondrial genomes have evolved remarkable diversity (Burger et al. 2003). Most mitochondria retain a genome, a remnant of an ancestral α-proteobacterial chromosome. It is usually organized on a multicopy, circular DNA molecule or a circularly permutated linear array that encodes genes for rRNAs, tRNAs, and proteins involved in the electron transport chain, ATP synthesis, and a few housekeeping functions (Burger et al. 2003). The most gene-rich mitochondrial genomes identified to date have been found in jakobids (Burger et al. 2013), whereas all other eukaryotes have gene complement reduced to varying extent (Gray et al. 2004). In several cases, for instance in the kinetoplastid flagellates, the mitochondrial genome has expanded into highly complex forms (Lukeš et al. 2005; Gray et al. 2010). Moreover, in several eukaryotic lineages including diplomonads, parabasalids, and microsporidians, the genome was lost altogether from their highly reduced organelles (Müller et al. 2012). The most reduced mitochondrial genomes are found in the alveolates, or more specifically the myzozoans, which include apicomplexans, dinoflagellates, and their relatives. Myzozoan mitochondrial genomes encode only subunits 1 and 3 of cytochrome *c* oxidase (*cox1* and *cox3*), one subunit of cytochrome *c* reductase (*cob*), and truncated but apparently functional fragments of small (SSU) and large subunit (LSU) mitoribosomal rRNA genes (Feagin et al. 1997; Nash et al. 2008; Waller and Jackson 2009). The gene coding for *cox2*, universally present in other mitochondrial genomes, has been split and transferred to the nucleus (Waller and Keeling 2006).

In apicomplexan parasites, mitochondrial genes are encoded on a linear molecule ranging in length from 5.8 kb in *Parahaemoproteus* to 11.0 kb in *Babesia*, which can be either monomeric or is composed of circularly permutated linear arrays (Feagin et al. 1997). In dinoflagellates, the

Article

Fast Track

mitochondrial genome is broken into small linear fragments containing genes with extensively edited transcripts, as well as many pseudogenes and apparently nonfunctional gene fragments (Imanian and Keeling 2007; Jackson et al. 2007; Kamikawa et al. 2007, 2009; Nash et al. 2007, 2008; Waller and Jackson 2009). The deep-branching relatives of dinoflagellates, *Perkinsus* and *Oxyrrhis*, lack RNA editing, and in the former species translational frame shifting is required for expression of its mitochondrial genes (Slamovits et al. 2007; Masuda et al. 2010; Zhang et al. 2011). Third major group of alveolates are the ciliates, which usually harbor a gene-rich (~50 genes) mitochondrial genome (Gray et al. 2004), with their anaerobic members featuring a reduced gene set (Akhmanova et al. 1998). The nature of mitochondrial genome of *Acavomonas peruviana*, a heterotrophic alveolate branching on the root of myzozoans, demonstrates that the ancestral state for myzozoan mitochondria was a linear chromosome with telomeric sequences at both ends (Janouškovec, Tikhonenkov, et al. 2013; Tikhonenkov et al. 2014).

Since the diversity of mitochondrial genomes of dinoflagellates and myzozoans allows reconstruction of a putative ancestral state, we wondered how informative the deep-branching relatives of apicomplexans will be in this respect. Since the discovery in 2008 of the coral-associated *Chromera velia* and the more recent description of related *Vitrella brassicaformis*, these photosynthetic algae have received much attention (Moore et al. 2008; Janouškovec et al. 2010; Woehle et al. 2011; Burki et al. 2012; Oborník et al. 2012; Janouskovec, Sobotka, et al. 2013; Oborník and Lukeš 2013; Petersen et al. 2014). While *Chromera* and *Vitrella* have been used to solve a few riddles about apicomplexan plastid genome evolution (Janouškovec et al. 2010; Janouskovec, Sobotka, et al. 2013), it remained unclear how their mitochondrial genomes compare to the equally unusual apicomplexan mitochondrion, which lacks some signature elements of the canonical mitochondrial metabolism. *Chromera* has been proposed to harbor just the *cox1* gene in its mitochondrion (Petersen et al. 2014). Here, we report the mitochondrial genomes and transcriptomes of *Chromera* and *Vitrella*, supplemented with the analysis of mitochondrial metabolic pathways based on the data from high-quality assemblies of their nuclear genomes (Pain A, Otto TD, Keeling PJ, Oborník M, Lukeš L, unpublished data), which reveal an unexpectedly altered respiratory chain in the former alga. The reduction of the respiratory chain found in the mitochondrion of *Chromera* is unprecedented in an aerobic eukaryote.

Results

Mitochondrial Genome of *Chromera*

We searched a high-quality whole-genome assembly and transcriptome, as well as an assembly derived from a mitochondrial DNA-enriched fraction (see Materials and Methods for details) for the five mitochondrial genes expected in the myzozoan lineage, namely *cox1*, *cox3*, *cob*, genes coding for SSU and LSU rRNAs, and other typical mitochondrial genes. We identified a single conserved gene coding for *cox1*, a highly divergent *cox3* gene, and numerous rRNA fragments. Although *cox1* can be easily found by BLAST search, *cox3* is too divergent to be detected by homology-based searching algorithms. However, when the mitochondrial sequences were investigated for the presence of open reading frames (ORFs), one ORF with about 250 amino acids of *cox3*-like sequence was identified as a putative *cox3* (see Materials and Methods for details). This gene contains 42% hydrophobic residues and seven predicted transmembrane segments (supplementary figs. S1 and S2, Supplementary Material online), and has a very weak sequence similarity with the *cox3* genes when investigated with hidden Markov model (HMM) searches. However, the percentage of hydrophobic residues, number of predicted transmembrane domains (six in cox3 of *Plasmodium*), presence of short motifs conserved in myzozoan cox3 proteins, and similar divergence of cox3 in dinoflagellates (see alignment in supplementary fig. S1, Supplementary Material online), all point to the fact that the gene identified in *Chromera* is *cox3*.

The *cob* gene, which was so far present in all other aerobic mitochondrial genomes, was surprisingly absent from all assemblies and raw reads from *Chromera*. Phylogenetic analysis of *cox1* shows the *Chromera* gene on a long branch with low support (bootstrap 38%, posterior probability [pp] 0.92) as a sister clade to the comparably divergent sequence from *Perkinsus*. The highly divergent *cox1* gene from *Vitrella* appears to be weakly related (bootstrap 45%, pp 0.99) to its *Oxyrrhis* homolog, both branching inside the highly supported myzozoan clade (supplementary fig. S3, Supplementary Material online). Analysis of total and mitochondrial DNA-enriched sequences also showed that the two protein-coding genes are found in multiple genomic contexts in the mitochondrion of *Chromera*. The full-length *cox1* genes are flanked by various sequences, and the same applies for a number of gene fragments (supplementary tables S1 and S2, Supplementary Material online), yet only a single full-length transcript is formed (fig 1*A*). The putative *cox3* is fused with an upstream *cox1* fragment (amino acids 1–192; supplementary table S2, Supplementary Material online) and, as shown by quantitative polymerase chain reaction (PCR), a fusion transcript is produced, which apparently undergoes a subsequent cleavage (fig. 1*A* and supplementary fig. S4, Supplementary Material online).

The mitochondrial genome of *Vitrella* contains a fused *cob-cox1* gene and a divergent *cox3* gene (supplementary fig. S5, Supplementary Material online). In *Chromera*, we have also identified expressed oligoadenylated rRNA gene fragments *rnl1*, *rnl8*, *rnl12*, *rns1*, *rns5*, and *rns7* (fig. 1*B* and *D*) previously found in myzozoans (Imanian and Keeling 2007; Slamovits et al. 2007; Nash et al. 2008; Waller and Jackson 2009). Multiple lines of evidence including electron microscopy of the mitochondrial DNA-enriched fraction (fig. 2) show that the *Chromera* mitochondrial DNA is composed of numerous, short linear molecules (supplementary fig. S6, Supplementary Material online). No indications of RNA editing have been found in the mitochondrial-encoded transcripts of *Chromera* and *Vitrella*.

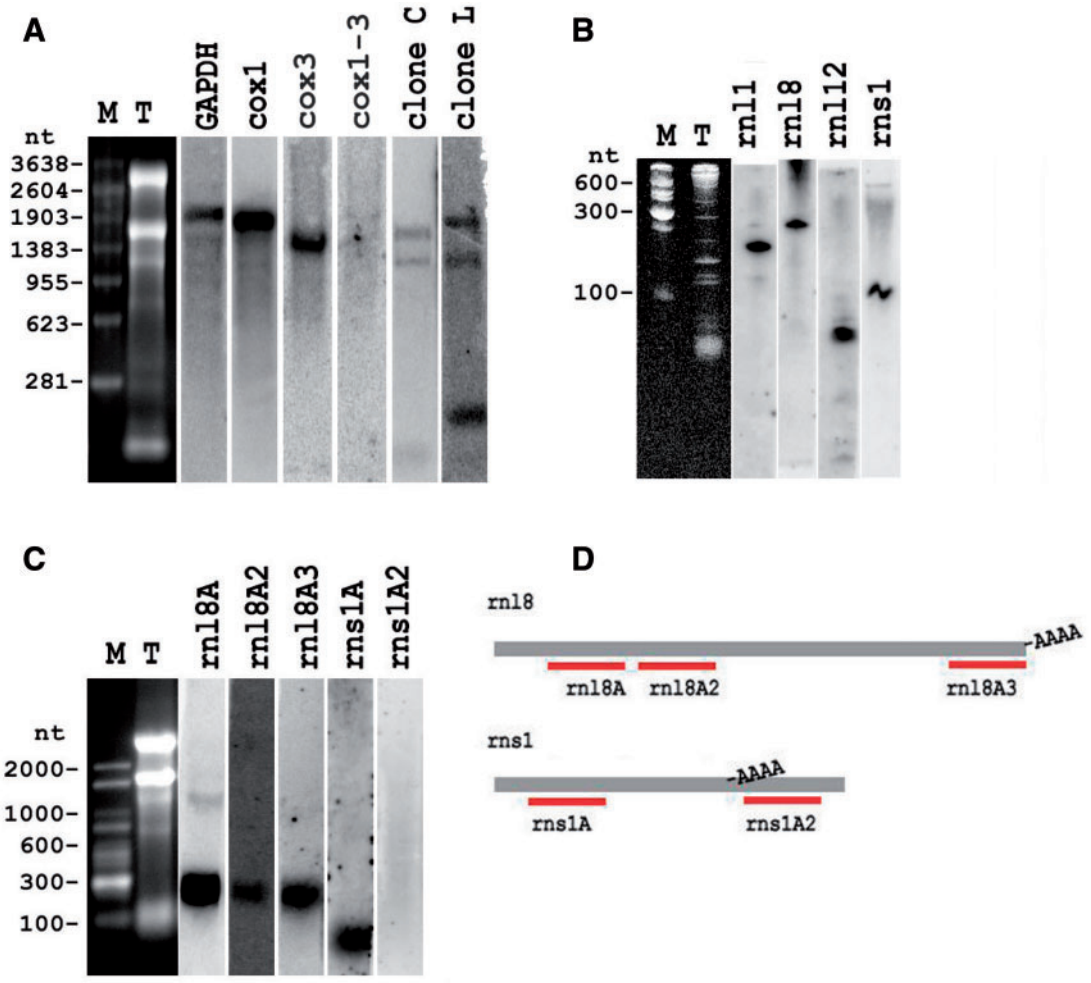

Fig. 1. Transcription pattern of *Chromera velia* nuclear and mitochondrial genes or gene fragments revealed by Northern blot analysis of total RNA. RNA was detected by γ-ATP radiolabeled antisense oligonucleotides. In panels (*A*–*C*), Ethidium bromide-stained gels with a marker (M) and total RNA (T) are shown to the left. (*A*) Transcripts of a nuclear glyceraldehyde-3-phosphate dehydrogenase gene, the *cox1* and *cox3* genes (mature transcripts), primary transcript of *cox3* containing a part of *cox1* (*cox1-3*), and regions flanking the *cox1* gene (clones C and L). (*B*) Transcripts of the mitochondrial rRNA gene fragments (*rnl1*, *rnl8*, *rnl12*, and *rns1*) resolved on a high resolution 5% polyacrylamide gel. (*C*) Transcription pattern of rRNA gene fragments *rnl8* (detected with oligonucleotides *rnl8A*, A2 and A3) and *rns1* (detected with oligonucleotides rns1A and A2), as revealed in a medium resolution 1% agarose gel. (*D*) Positions of labeled oligonucleotides are marked with bars; polyadenylation sites, indicated as -AAAA, were determined by 3′-polyA RACE.

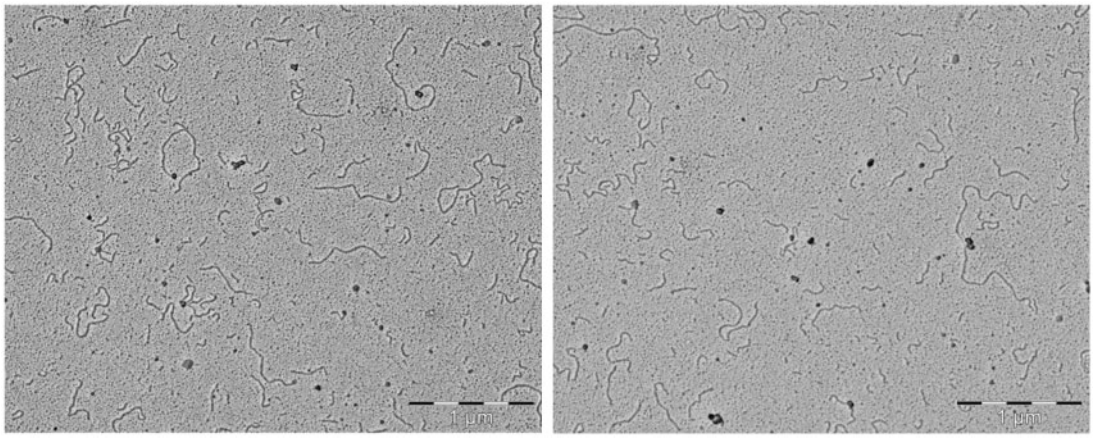

Fig. 2. Electron microscopy of the *Chromera velia* mitochondrial DNA prepared from fractions H1 and H2 obtained from ultracentrifugation of total DNA in the CsCl-Hoechst 33258 gradient (see supplementary fig. S14, Supplementary Material online) and examined in a transmission electron microscope as described previously (Yurchenko et al. 1999).

Respiratory Chain of *Chromera*

Searching for the nuclear-encoded subunits of the respiratory chain did not identify any traces of proteins associated with complexes I (NADH: ubiquinone oxidoreductase) and III (ubiquinol: cytochrome *c* oxidoreductase). In contrast, subunits of complexes II (membrane-bound succinate dehydrogenase) and IV (cytochrome *c* oxidase), ATP synthase, and most enzymes associated with the respiratory chain in the related apicomplexans and dinoflagellates (electron-transfer flavoprotein, alternative NADH dehydrogenases, alternative oxidase [AOX], soluble fumarate reductase, etc.) (Danne et al. 2013) were found in the nuclear genome of *Chromera* (fig. 3*A* and table 1).

Detailed reconstruction of the *Chromera* metabolism revealed that the entire respiratory chain and associated pathways are uniquely divided into two independently operating

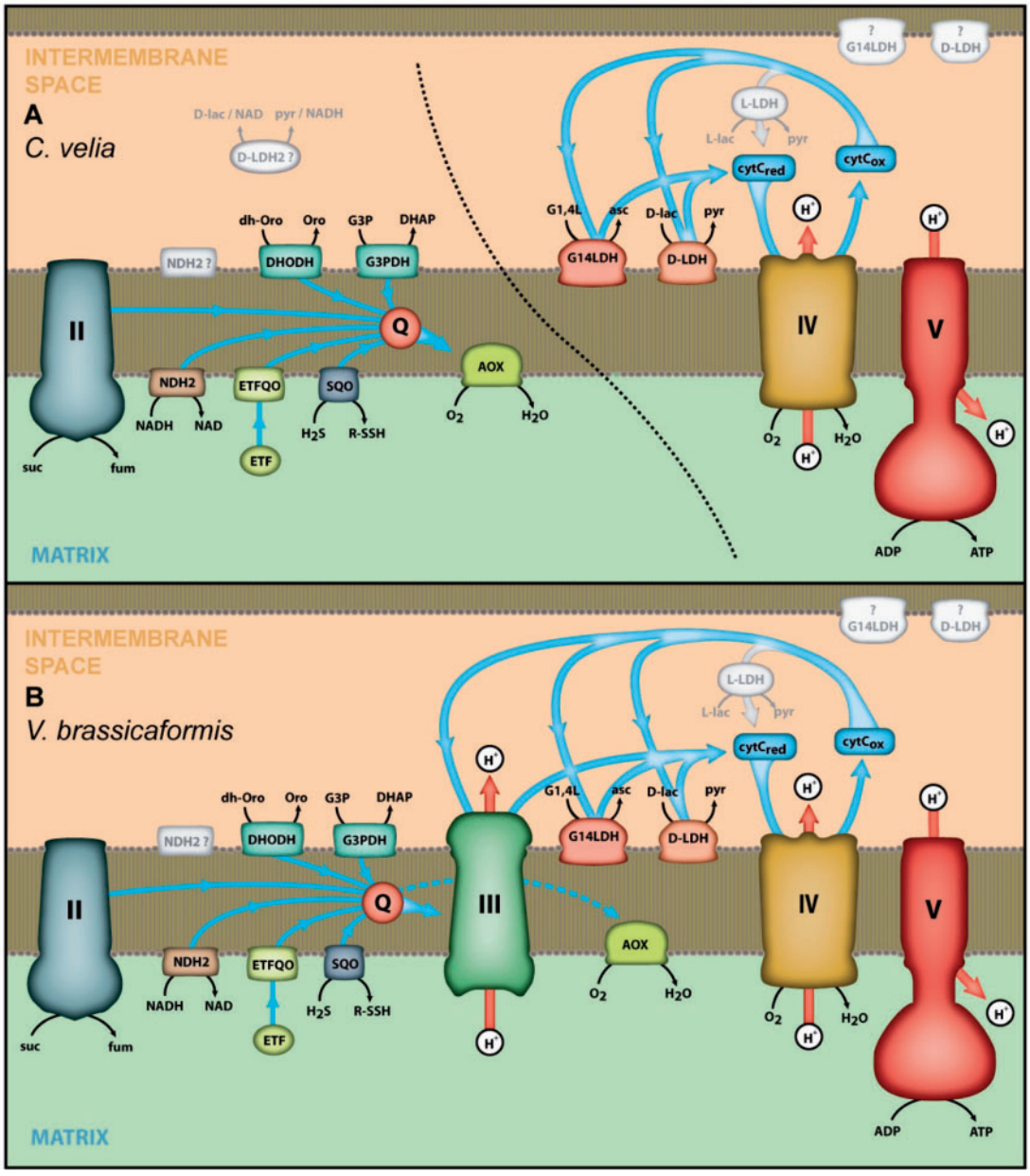

Fig. 3. The reconstructed respiratory chains in (*A*) *Chromera velia* and (*B*) *Vitrella brassicaformis*. Protein localization is shown based on predicted targeting and on available data. Proteins with alternative or uncertain localization are indicated in gray with a question mark. In *Chromera* the respiratory chain is split into two disconnected parts. Complex II, alternative NADH dehydrogenase (NDH2), glycerol 3-phosphate dehydrogenase (G3PDH), ETFQO, and other enzymes are donating electrons to ubiquinone, which passes them to AOX. D-Lactate:cytochrome *c* oxidoreductase (D-LDH), L-lactate:cytochrome *c* oxidoreductase (L-LDH, also known as cytochrome b_2), and L-galactono-1,4-lactone dehydrogenase (G14LDH) are donating electrons to soluble cytochrome *c*, which is oxidized by cytochrome *c* oxidase (complex IV). The NADH-dependent D-lactate dehydrogenase (D-LDH2) recycles pyruvate, generated by the cytochrome-dependent D-LDH and L-LDH, into lactate, and consumes NADH. The respiratory chain of *Vitrella* is continuous, with alternative ubiquinone reductases, D-LDH, L-LDH, and G14LDH also present. However, D-LDH2 is absent and AOX lacks a robust mitochondrial import signal. The complexes are not depicted to scale.

Table 1. Respiratory Chain Components and Other Enzymes Typical for Anaerobic Species in *Chromera* and *Vitrella*, in Apicomplexan, Dinoflagellate, and Perkinsid Data Sets.

Name	Common Abbreviation	EC Number	Respiratory Chain Complex or Metabolic Process	chromerids				Apicomplexa						Perkinsea	*Oxyrrhis*	Dinophyceae: Gonyaulacales
				Chromera proteome	*Chromera* transcriptome	*Chromera* genome	*Vitrella* transcriptome	*Vitrella* genome	*Eimeria*	*Cryptosporidium*	*Neospora /Toxoplasma*	*Babesia /Theileria*	*Plasmodium*	*Perkinsus marinus*	*Oxyrrhis marina*	*Lingulodinium*
NADH dehydrogenase		1.6.5.3	Complex I													
Mitochondrial alternative NADH dehydrogenase		1.6.5.9	NADH dehydrogenase	•	•	3	•	5	3	1	2	1	1			•
Electron transfer flavoprotein	ETF		Alternative UQ Reductases	•	•	1	•	2			1			•	•	•
Electron transfer flavoprotein:ubiquinone oxidoreductase	ETFQO	1.5.5.1		•	•	1	•	1			1					
Glycerol 3-phosphate:ubiquinone oxidoreductase	G3P DH	1.1.5.3		•	•	1	•	1	1		1	1	1	•		•
Sulfide:ubiquinone oxidoreductase*		1.8.5.4		•	•	1	•	2							•	
Dihydroorotate:ubiquinone oxidoreductase	DHODH	1.3.5.2		•	•	1	•	1	1		1	1	1			
Ubiquinone biosynthesis enzymes	UbiA, UbiE, UbiG, UbiH	2.5.1.-, 2.1.1.201, 2.1.1.222, 1.14.13.-	Ubiquinone biosynthesis	•	•	•	•	•	•	•	•	•	•	•		•
Succinate dehydrogenase		1.3.5.1	Complex II	•	•	•	•	•	•		•	•	•	•	•	•
Soluble fumarate reductase*		1.3.1.6	Fumarate reductase	•	•	3								•	•	•
Alternative oxidase*	AOX	1.10.3.11	Alternative oxidase	•	•	2	•	3		1				•		•
Cytochrome *b*	cob	1.10.2.2	Complex III				•	1	1		1	1	1		•	•
Cytochrome *c1*	cytC1	1.10.2.2					•	1	1		1	1	1	•	•	•
Mitochondrial Rieske protein		1.10.2.2					•	1	1		1	1	1	•	•	•
14 kDa protein		1.10.2.2					•	1	1		1	1	1		•	•
Hinge subunit		1.10.2.2					•	1			1	1	1	•		•
Cytochrome c1 heme lyase		4.4.1.17	Complex III assembly				•	1				1	1			
L-Lactate dehydrogenase (cytochrome) (cytochrome *b2*)		1.1.2.3	Alternative cytochrome *c* reductases	•	•	2	•	2						•	•	•
D-Lactate dehydrogenase (cytochrome)		1.1.2.4		•	•	2	•	2								
L-Galactonolactone dehydrogenase	G14LDH	1.3.2.3		•	•	1	•	1								
Glucose-methanol-choline oxidoreductase		1.1.5.2; 1.1.2.7; 1.1.99.1			•	3					1				•	•
Cytochrome *c*			Cytochrome *c*	•	•	•	•	•	•		•	•	•		•	•
Cytochrome *c* oxidase		1.9.3.1	Complex IV	•	•	•	•	•	•		•	•	•	•	•	•
ATP synthase		3.6.3.14	Complex V	•	•	•	•	•	•		•	•	•	•	•	•
Glycolytic enzymes			Glycolysis	•	•	•	•	•	•	•	•	•	•	•	•	•
Pyruvate:orthophosphate dikinase*		2.7.9.1			•	2	•	2		1						
2-Oxoglutarate dehydrogenase*	OGDH	1.2.4.2	TCA	•	•	1	•	1	1		1	1	1			•

(continued)

Table 1. Continued.

Name	Common Abbreviation	EC Number	Respiratory Chain Complex or Metabolic Process	chromerids					Apicomplexa					Perkinsea	*Oxyrrhis*	Dinophyceae: Gonyaulacales
				Chromera proteome	*Chromera* transcriptome	*Chromera* genome	*Vitrella* transcriptome	*Vitrella* genome	*Eimeria*	*Cryptosporidium*	*Neospora /Toxoplasma*	*Babesia /Theileria*	*Plasmodium*	*Perkinsus marinus*	*Oxyrrhis marina*	*Linguodinium*
Aconitase		4.2.1.3		•	•	3	•	2	2		1	1	1			•
Citrate synthase*		2.3.3.1		•	•	4	•	4	2		3	1	1	•	•	•
Fumarase*		4.2.1.2		•	•	1	•	1	1		1	1	1	•		•
Isocitrate dehydrogenase (NAD)		1.1.1.41		•	•	1	•	1								•
Isocitrate dehydrogenase (NADP)		1.1.1.42		•	•	2	•	2	2		2	1	1	•	•	•
Malate dehydrogenase*	MDH	1.1.1.37		•	•	1	•	2[a]	1	1	1		1	•		
Succinyl-CoA synthetase (succinate-CoA ligase, GDP or ADP-forming)*		6.2.1.4-5		•	•	1	•	1	1		1	1	1	•	•	•
Phosphoenolpyruvate carboxykinase (ATP)*	PEPCK-ATP	4.1.1.49	Fermentation pathways		•	1	•	1	1		2	1	1	•	•	•
Phosphoenolpyruvate carboxykinase (GTP)*	PEPCK-GTP	4.1.1.32			•	2										
Pyruvate carboxylase		6.4.1.1		•	•	2	•	1			1				•	•
Malic enzyme*		1.1.1.38-40		•	•	3	•	3		1				•		•
D-Lactate dehydrogenase*	D-LDH	1.1.1.28		•		1										•
L-Lactate dehydrogenase*	L-LDH	1.1.1.27					•	3	1	1	2	1	1			
Pyruvate decarboxylase*		4.1.1.1			•	1	•	2		1						
Acetaldehyde/alcohol dehydrogenase*	AADH, AdhE	1.1.1.1; 1.2.1.10			•	1	•	1		2						
Alcohol dehydrogenase, NAD-dependent*	Fe-ADH	1.1.1.1		•	•	2	•	1	1		1			•	•	•
Pyruvate dehydrogenase complex*	PDC	1.2.4.1		•	•	1	•	1	1		1		1			
Pyruvate:NADP oxidoreductase*	PNO	1.2.1.51		•	•	1	•	1		1				•		•
Pyruvate:formate lyase*	PFL	2.3.1.54		•	•	1	•	1								
Pyruvate:formate lyase activating enzyme*	PFL-AE	1.97.1.4					•	1								
Acetate:succinate CoA-transferase*	ASCT	2.8.3.18		•	•	1										
Acetyl-CoA synthetase, ADP forming (acetate-CoA ligase)*		6.2.1.13			•	1	•	2					1			
Acetyl-CoA synthetase, AMP forming (acetate-CoA ligase)		6.2.1.13		•	•	2	•	3	1	1	2	1	1	•	•	•
Phosphate acetyl transferase (phosphotransacetylase)*	PTA	2.3.1.8												•	•	•
Acetate kinase*		2.7.2.1												•		•
Propionate:succinate CoA-transferase*		2.8.3.-		•	•	1										
Propionyl-CoA carboxylase*		6.4.1.3		•		1	•	1								
[FeFe] Hydrogenase maturase HydE*	HydE		Hydrogenase		•	1	•	1								
[FeFe] Hydrogenase maturase HydF*	HydF					1	•	1								
[FeFe] Hydrogenase maturase HydG*	HydG				•	1	•	1								

(continued)

Table 1. Continued.

Name	Common Abbreviation	EC Number	Respiratory Chain Complex or Metabolic Process	chromerids				Apicomplexa					Perkinsea		*Oxyrrhis*	Dinophyceae: Gonyaulacales
				Chromera proteome	*Chromera* transcriptome	*Chromera* genome	*Vitrella* transcriptome	*Vitrella* genome	*Eimeria*	*Cryptosporidium*	*Neospora /Toxoplasma*	*Babesia /Theileria*	*Plasmodium*	*Perkinsus marinus*	*Oxyrrhis marina*	*Lingulodinium*
[FeFe] Hydrogenase*		1.12.7.2			•	1	•	1		1						•
Nuclear prelamin A recognition factor-like protein	NARFL				•	1	•	1	1	1	1	1	1			
Coenzyme F420 hydrogenase		1.12.98.1				1									•	
Alpha-ketoacyl reductase*		1.1.1.100	Various proteins	•	•	3	•	1	1		2		1	•		•
Alpha-ketoacyl synthase*		2.3.1.41		•	•	11	•	8	2	2	3		1			
NAD(P)H:ferredoxin oxidoreductase*		1.18.1.2			•	1	•	1		1	1	1	1			•
Flavodiiron protein*															•	
NADH oxidase		1.6.3.4				1										
Nitrite reductase*		1.7.1.4			•	1	•	1			1	1				
Sulphite reductase		1.8.1.2		•	•	1	•	1								•
Alanine racemase*		5.1.1.1			•	1	•	1	1	1	1			•		
Alanine aminotransferase*	ALAT	2.6.1.2		•	•	1	•	3	1		1			•	•	•
Aspartate aminotransferase*	ASAT	2.6.1.1		•	•	1	•	3	1		1	1	1	•		•
Glutamate dehydrogenase*	GLDH	1.4.1.2		•	•	1	•	1	1		1	1	2	•	•	•
Opine dehydrogenases*		1.5.1.28; 1.5.1.17; 1.5.1.22; 1.5.1.11			•	3	•	4	1		1					•

NOTE.—A number of paralogs detected in each genome is shown, and presence/absence only is shown for transcriptomic or proteomic data (presence is denoted by a filled circle). If proteins show strong evidence of lateral gene transfer from bacteria (data not shown), the respective cells are boxed. Commonly used abbreviations and EC numbers are shown, when applicable. Phylogenetic patterns of protein occurrence are color-coded in the following way: orange, proteins lost in *Chromera* only; light-green, proteins occurring exclusively in *Chromera* (proteins found in *Chromera* and in dinoflagellates/perkinsids are included into this group as well, as transcriptomic data cannot robustly demonstrate absence of a certain protein, the same applies to all groups below); blue-green, proteins occurring in both *Chromera* and *Vitrella*; gray, in *Chromera*, *Vitrella*, and in *Cryptosporidium*, a mitosome-bearing apicomplexan; violet, in *Chromera*, *Vitrella*, and apicomplexans (but lost in at least 2 of 5 major apicomplexan lineages); pink, in dinoflagellates/perkinsids only.

[a]Only one malate dehydrogenase homolog in Vitrella originates from a bacterial source via lateral gene transfer.

*Enzymes of anaerobic energy metabolism in eukaryotes, according to Müller et al. 2012 and Ginger et al. 2010.

subchains (fig. 3*A* and table 1).The initial subchain is represented by alternative NADH dehydrogenases, which substitute for the electron transport function of the lost complex I. Electrons from alternative NADH dehydrogenases, complex II, electron-transfer flavoprotein: ubiquinone oxidoreductase (ETFQO), and other donors (fig. 3*A* and table 1) are channeled to ubiquinone, which passes them to alternative oxidase (AOX), an electron sink, without any consequent proton pumping and link to the respiration whatsoever. Our model proposes that complex IV and ATP synthase operate independently (fig. 3*A*), with complex IV being the only complex that is able to pump protons into the mitochondrial intermembrane space and form a membrane potential. Orthologs of both L- and D-lactate: cytochrome *c* oxidoreductases were identified in the nuclear genome (see Materials and Methods for additional details). These proteins are supposed to mediate the transfer of electrons unidirectionally from lactate to cytochrome *c*, thus uniquely bypassing the missing complex III (fig. 3*A*). Analysis of L-lactate: cytochrome *c* oxidoreductases shows that in eukaryotes these genes have an extremely patchy phylogenetic distribution, as they are present in fungi, some dinoflagellates, *Perkinsus*, *Chromera* (2 genes), and *Vitrella* (2 genes; see alignment in supplementary fig. S7, Supplementary Material online). Phylogenetic analysis of D-lactate: cytochrome *c* oxidoreductases reveals a complex evolutionary history, as the gene from *Chromera* clusters with high support along with fungal homologues in the eukaryotic clade (fungi, plants, *Ectocarpus*, amebae, and rhodophytes; see supplementary fig. S8, Supplementary Material online). In addition to this clade, other eukaryotes appear in the company of various bacteria. However, none of these bacterial-derived clades contains the *Chromera* sequence.

Regeneration of lactate from pyruvate is accomplished by a bidirectional NADH-dependent D-lactate dehydrogenase of likely ancient eukaryotic origin (fig. 4 and table 2). The canonical conversion of lactate to pyruvate via a NADH-dependent L-lactate dehydrogenase is missing from *Chromera*, although the canonical enzyme is present in *Vitrella* and the apicomplexans (table 1). This suggests that the common ancestor of apicomplexans, *Chromera* and *Vitrella*

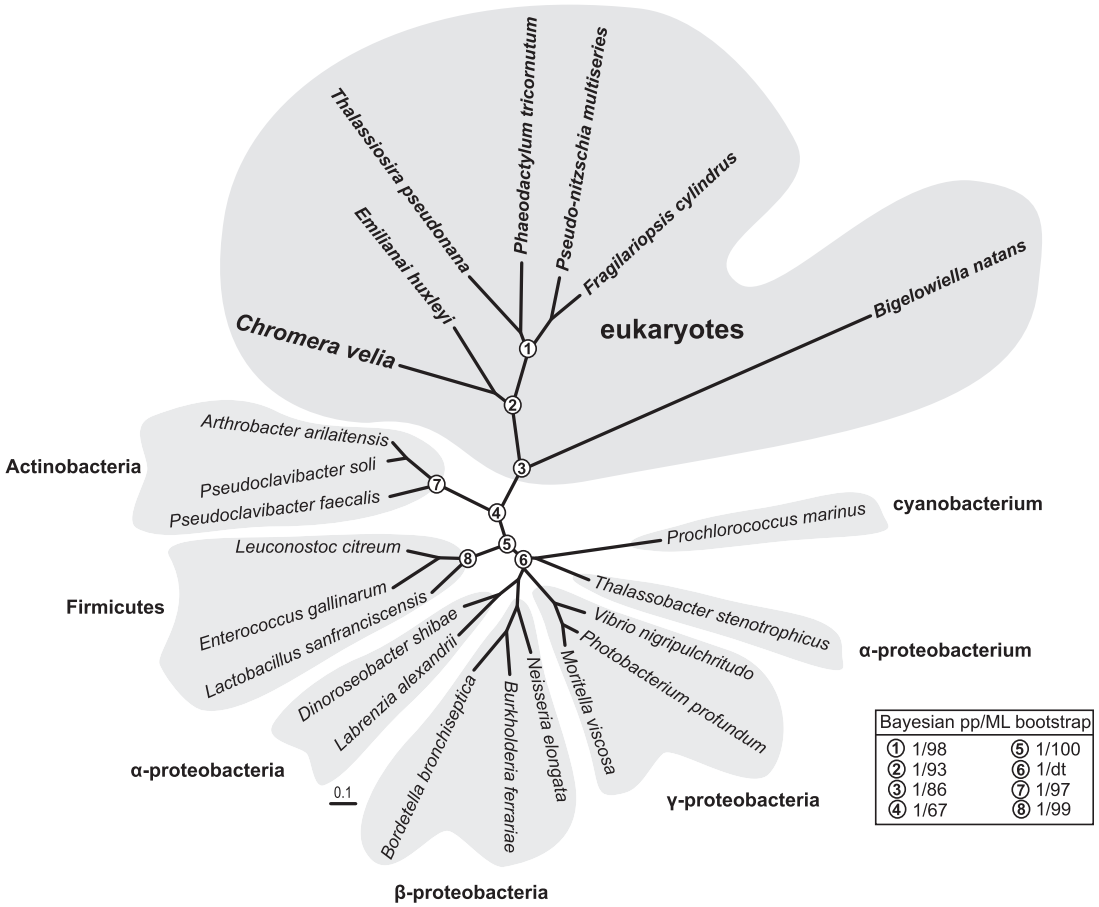

Fig. 4. A ML phylogenetic tree including *Chromera velia* NADH-dependent D-lactate dehydrogenase (D-LDH2), with its eukaryotic and bacterial orthologs. Bayesian PP/ML bootstraps are in the table. Accession number of sequences in the tree: Fracy1_207885; Psemu1_183545; Phatr2_46664; Thaps3_268453; EMIHUDRAFT_450888; Bigna1_67620 (sequences downloaded from JGI http://jgi.doe.gov/); WP_012178639.1; WP_008193115.1; WP_033467713.1; WP_028227993.1; WP_003774459.1; CED58655.1; WP_011218908.1; WP_022589137.1; KGK78572.1; WP_012195855.1; WP_004902775.1; WP_029486096.1; WP_014082344.1; WP_013349576.1; WP_028245171.1; WP_019617597.1 (sequences downloaded from NCBI http://www.ncbi.nlm.nih.gov/).

Table 2. Putative Localizations of Enzymes of Interest Predicted with the TargetP, SignalP, and MitoProt Programs.

Gene ID	Enzyme Name	Signal Peptide	Length, aa	Transit Peptide (uncut signal peptide)	Length, aa	Transit Peptide (cut signal peptide)	Length, aa	MitoProt II
Cvel_24584.t1	NADH-dependent D-lactate dehydrogenase	S 0.986	18	S 0.149	18	M 0.525	19–48	0
Vbra_2211.t1	NADH-dependent L-lactate dehydrogenase	0	0	0	0	0	0	0
Vbra_4978.t1	NADH-dependent L-lactate dehydrogenase	0	0	C 0.292 / M 0.225	5	0	0	0
Vbra_16839.t1	NADH-dependent L-lactate dehydrogenase	0	0	0	0	0	0	0
Cvel_6082.t1	D-Lactate: cytochrome *c* oxidoreductase	S 0.941	17	C 0.561	13	M 0.815	18-24	0.8995
Cvel_20317.t1	D-Lactate: cytochrome *c* oxidoreductase	Anch 0.587	46	C 0.759/ M 0.706	52	C 0.759 M 0.706	1–52	0.9959
Vbra_3212.t1	D-Lactate: cytochrome *c* oxidoreductase	S 0.315	21	M 0.796	93	M 0.796	1–93	0.9946
Vbra_9909.t1	D-Lactate: cytochrome *c* oxidoreductase	0	0	M 0.806	18	0	0	0.8978
Cvel_4425.t1	L-Lactate: cytochrome *c* oxidoreductase	0	0	0	0	0	0	0
Cvel_5763.t1	L-Lactate: cytochrome *c* oxidoreductase	0	0	0	0	0	0	0
Vbra_7868.t1	L-Lactate: cytochrome *c* oxidoreductase	0	0	0	0	0	0	0
Vbra_19079.t1	L-Lactate: cytochrome *c* oxidoreductase	0	0	0	0	0	0	0
Vbra_2234.t1	Galacto-1,4-lactone: cytochrome *c* oxidoreductase	S 0.993	21	M 0.595	55	M 0.900	22–56	0.9863
Cvel_9992.t1	Galacto-1,4-lactone: cytochrome *c* oxidoreductase	S 0.999	27	S 0.794	27	M 0.738	24–54	0
Cvel_6529.t1	Alternative oxidase	0	0	M 0.913	35	0	0	0.9747
Cvel_21608.t1	Alternative oxidase	S 0.575	34	M 0.849	29	0	0	0.9918
Vbra_7072.t1	Alternative oxidase	S 0.635	30	M 0.782	38	0	0	0.966
Vbra_14859.t1	Alternative oxidase	S 0.843	23	M 0.578	57	C 0.588 M 0.602	24–57	0.9786
Vbra_15987.t1	Alternative oxidase	S 0.848	35	M 0.544	45	0	0	0.9836
Cvel_3201.t1	Alternative NADH dehydrogenase	0	0	0	0	0	0	0
Cvel_12889.t1	Alternative NADH dehydrogenase	0	0	0	0	0	0	0
Cvel_17721.t1	Alternative NADH dehydrogenase	S 1.000	18	M 0.411	41	M 0.824	19–41	0.951
Vbra_528.t1	Alternative NADH dehydrogenase	0	0	0	0	0	0	0
Vbra_4873.t1	Alternative NADH dehydrogenase	S 0.998	24	C 0.189 / M 0.134 / S 0.153	20	C 0.795	25–75	0.9844
Vbra_8108.t1	Alternative NADH dehydrogenase	0	0	0	0	0	0	0
Vbra_13793.t1	Alternative NADH dehydrogenase	S 0.997	25	S 0.608	19	C 0.850	20–62	0.709
Vbra_21650.t1	Alternative NADH dehydrogenase	S 1.000	24	S 0.869	23	C 0.965	24–54	0.6591
Vbra_21162.t1	Glycerol 3-phosphate dehydrogenase	S 0.812	25	M 0.721	111	0	0	0.4891
Cvel_27966.t1	Glycerol 3-phosphate dehydrogenase	S 0.492	25	M 0.872	82	0	0	0.8563
Cvel_25193.t1	Dihydroorotate: ubiquinone oxidoreductase	S 0.986	24	S 0.698	23	S 0.510	17	0
Vbra_7220.t1	Dihydroorotate: ubiquinone oxidoreductase	Anch 0.717	44	0	0	0	0	0
Cvel_9173.t1	Electron transfer flavoprotein ubiquinone oxidoreductase	0	0	M 0.732	52	—	—	0.9261
Vbra_4697.t1	Electron transfer flavoprotein ubiquinone oxidoreductase	0	0	0	0	0	0	0
Cvel_17813.t1	Sulfide: ubiquinone oxidoreductase	S 0.906	28	M 0.439	42	0	0	0.1324
Vbra_5597.t1	Sulfide: ubiquinone oxidoreductase	0	0	M 0.614	109	0	0	0.7835
Vbra_15197.t1	Sulfide: ubiquinone oxidoreductase	S 0.999	17	C 0.247	64	C 0.795	47	0.3424

NOTE.—S, ER signal peptide; C, chloroplast transit peptide; M, mitochondrial transit peptide; Anch, signal anchor (transmembrane domain).

possessed both enzymes. Phylogenetic analysis shows that the unique bidirectional NADH-dependent D-lactate dehydrogenase clusters with its homologs from various diatoms, the coccolithophore *Emiliania huxleyi* and the chlorarachniophyte *Bigelowiella natans*, forming a separate clade from bacterial sequences (fig. 4). This suggests that the bidirectional NADH-dependent D-lactate dehydrogenase may have been present in the ancestor of the SAR supergroup (Stramenopiles, Alveolata, Rhizaria) and was differentially lost from some of its descendants. It also appears that organisms using this enzyme lack the canonical NADH-dependent L-lactate dehydrogenase.

We have also performed phylogenetic analyses of the following alternative ubiquinone reductases in the respiratory chains of *Chromera* and *Vitrella* (fig. 3): alternative NADH dehydrogenase (NDH2; fig. 5), ETFQO (supplementary fig. S9, Supplementary Material online), glycerol-3-phosphate dehydrogenase or glycerol-3-phosphate: ubiquinone oxidoreductase (G3PDH; fig. 6 and supplementary fig. S10, Supplementary Material online), dihydroorotate: ubiquinone oxidoreductase (DHODH; supplementary fig. S11, Supplementary Material online), sulfide: ubiquinone oxidoreductase (SQO; supplementary fig. S12, Supplementary Material online), and of another alternative cytochrome *c* reductase, galacto-1,4-lactone: cytochrome *c* oxidoreductase (G14LDH; supplementary fig. S13, Supplementary Material online). Most of the investigated enzymes, particularly NDH2 (fig. 5), G3PDH (fig. 6), ETFQO (supplementary fig. S9, Supplementary Material online), and G14LDH (supplementary fig. S13, Supplementary Material online) show possible ancient eukaryotic origins, since in these tress eukaryotes form a distinct clade, separate from α-proteobacteria or cyanobacteria. We cannot, however, exclude some horizontal gene transfer from unspecified bacteria to an ancient eukaryote. NDH2 from *Chromera* and *Vitrella* appears within a clade composed of eukaryotes with plastid. Because hosts of primary and secondary plastids constitute this clade, we suppose these genes originated in the primary host nucleus (nucleus of the algal endosymbiont in secondary endosymbiosis); genes in this large clade likely passed through several duplication events (fig. 5). However, one additional gene from *Vitrella*, which is absent from *Chromera*, appears among apicomplexan parasites, branching specifically with coccidians in a clade supposed to originate from secondary host (exosymbiont) nucleus (fig. 5). The phylogeny of G3PDH (fig. 6 and supplementary fig. S10, Supplementary Material online) shows the branching of *Chromera* and *Vitrella*, as well as *Perkinsus* in a sister position to apicomplexan parasites in frame of eukaryotes. The ETFQO tree displays similar grouping with *Chromera* and *Vitrella* genes sitting among homologs from alveolates (supplementary fig. S9, Supplementary Material online). Because G14LDH is absent from apicomplexans, its sister position to kinetoplastid flagellates has, due to the limited taxon sampling, no phylogenetic relevance (supplementary fig. S13, Supplementary Material online). We can only conclude that *Chromera* and *Vitrella* carry G14LDH of eukaryotic origin.

The second group of trees, in particular DHODH and SQO, show possible horizontal gene transfer from a bacterial donor. The SQO from *Chromera*, *Vitrella* and the centric diatom *Thalassiosira pseudonana* branch between Aquificales and α-proteobacteria (supplementary fig. S12, Supplementary Material online). Another SQO homolog from *Vitrella*, which is absent from *Chromera*, is branching among various fungi; however, the clade also contains homologs from *Tetrahymena* and *Nannochloropsis* (supplementary fig. S12, Supplementary Material online). Both *Chromera* and *Vitrella* contain two genes coding for DHODH: one is branching together with Apicomplexa and other eukaryotes with high support (supplementary fig. S11, Supplementary Material online). This gene is probably of mitochondrial origin because α-proteobacteria (together with γ-proteobacteria) cluster on the root of this eukaryotic clade. The second gene appears in a sister position to distant homologs from *Prunus* and a haptophyte, all sitting nonspecifically among bacterial sequences (supplementary fig. S11, Supplementary Material online).

In contrast to *Chromera*, the putative respiratory chain of *Vitrella* is similar to that found in apicomplexans. However, it also contains L- and D-lactate: cytochrome *c* oxidoreductases and NADH-dependent L-lactate dehydrogenase, whereas NADH-dependent D-lactate dehydrogenase is missing (fig. 3*B*). To confirm the absence of functional complex III, *Chromera* and *Vitrella* were incubated with a specific inhibitor of this respiratory complex, the fungicide azoxystrobin (Balba 2007). It should be noted that *Chromera* grows much faster than *Vitrella* and the latter alga forms large cell aggregations, which makes individual cells uncountable. For this reason, when evaluating the comparative effect of azoxystrobin on both algae, cumulative weight was used instead of growth curves to quantify the cultures. As shown in figure 7*C*, growth of *Vitrella* was inhibited, whereas *Chromera* remained unaffected even by very high concentrations of the drug. Growth curves also demonstrate that cyanide (KCN), a potent inhibitor of complex IV, killed *Chromera* (fig. 7*A*). Similarly, exposure to salicylhydroxamic acid (SHAM), an inhibitor of AOX, resulted in growth inhibition under a prolonged incubation (fig. 7*A*). However, when an inhibitory effect on respiration by SHAM was investigated in a short time frame of 4 min, no decline of respiration was recorded (fig. 7*B*).

Discussion

Four respiratory complexes and the proton-driven ATP-synthase perform core mitochondrial functions that are dispensable only in anaerobic or sugar-rich environments, often as a consequence of parasitism (Müller et al. 2012). Indeed, any major modifications to the respiratory chain are generally infrequent and almost exclusively associated with anaerobes. Only a few cases of its reduction have been encountered in aerobic eukaryotes. The respiratory complex I is missing from the mitochondrion of *Plasmodium* spp. and other apicomplexans (van Dooren et al. 2006; Vaidya and Mather 2009; Sheiner et al. 2013), as well as from some fungi (e.g., *Saccharomyces*) where alternative NADH dehydrogenases substitute its electron transfer function (Marcet-Houben et al. 2009). A pattern common to many eukaryotic

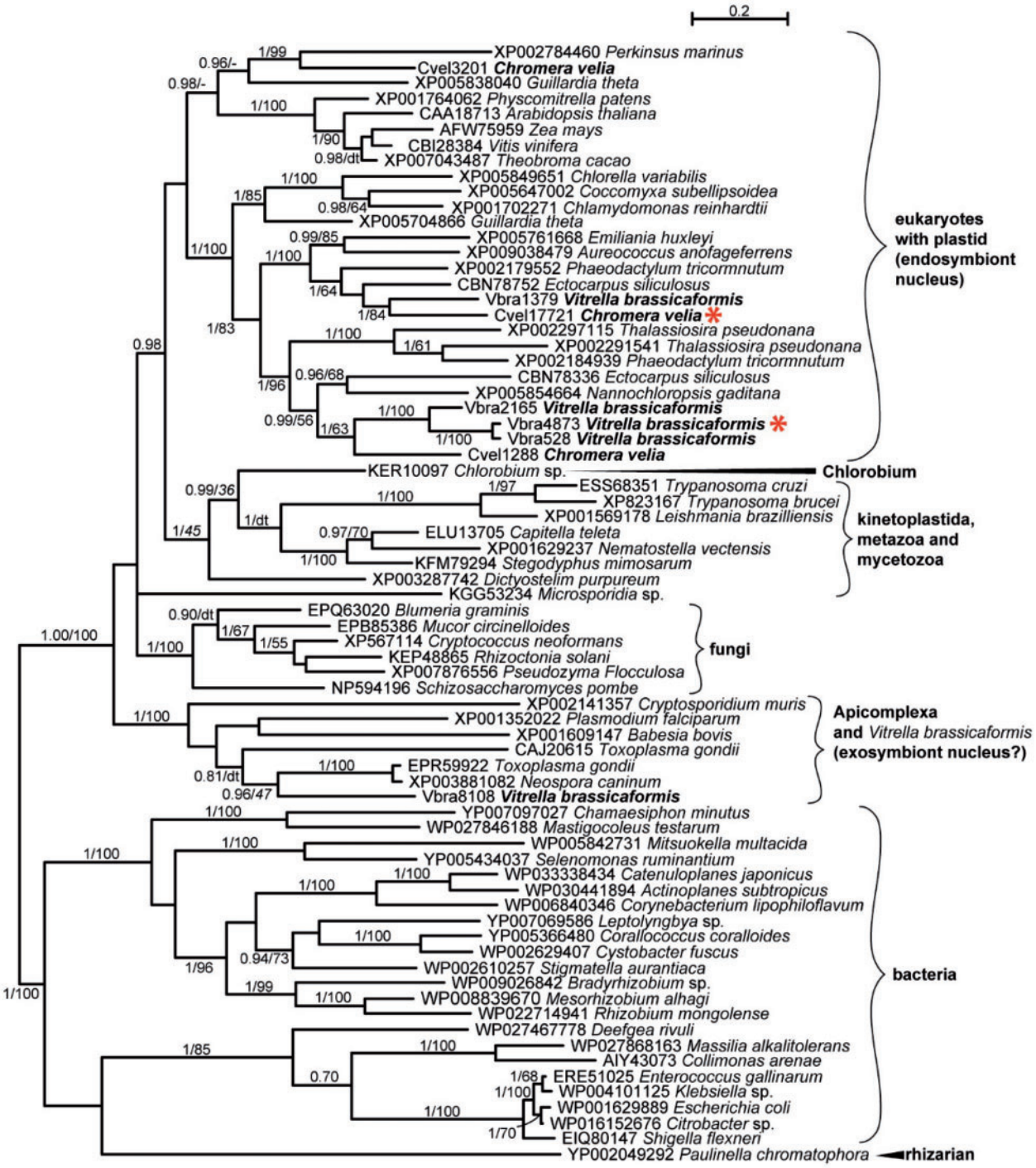

FIG. 5. Bayesian phylogenetic tree as inferred from alternative NADH dehydrogenase amino acid sequences. Proteins from *Chromera* and *Vitrella*, which are supposed to be involved in the respiratory chain are marked by *. Numbers above branches indicate Bayesian PP/ML bootstrap support (1,000 replicates).

anaerobes is the concurrent loss of complexes III and IV, while complexes I, II, and V have been retained, yet act in a different way: complex I donates electrons to rhodoquinone, which passes them to a membrane-bound fumarate reductase, whereas complex II-like enzymes operate in reverse, producing succinate (Müller et al. 2012). This type of respiratory chain occurs in anaerobic stages of some parasitic metazoans (a fluke *Fasciola* and a roundworm *Ascaris*), in marine benthic species experiencing periods of severe anoxia (a mussel *Mytilus* and an annelid *Arenicola*) and in an excavate alga *Euglena gracilis* grown in anaerobic conditions (Müller et al. 2012). Complexes III and IV were lost secondarily from the plant-pathogenic kinetoplastid *Phytomonas*, likely as a result of a deletion in the mitochondrial genome and subsequent adaptation to the sugar-rich environment of plant sap (Porcel et al. 2014). A similar pattern involving the loss of complexes

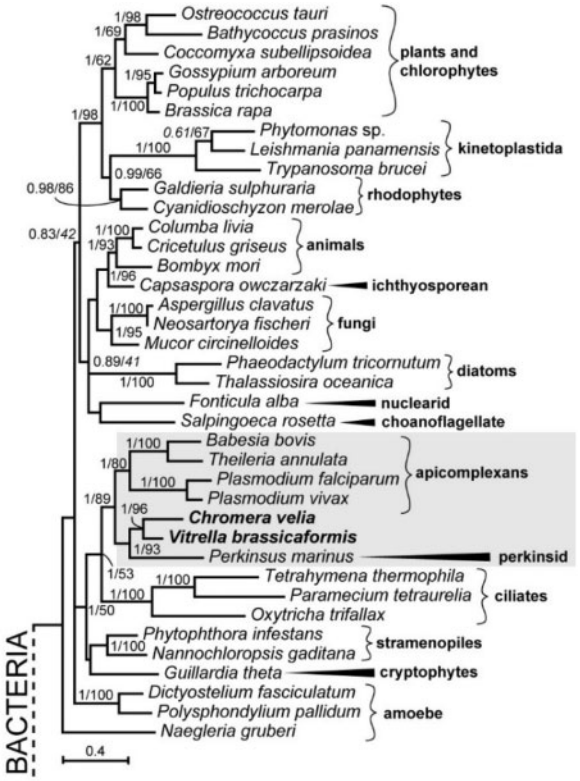

Fig. 6. A part of the Bayesian phylogenetic tree as inferred from glycerol-3-phosphate dehydrogenase amino acid sequences (see full tree in supplementary fig. S10, Supplementary Material online). Numbers above branches indicate Bayesian PP/ML bootstrap support (1,000 replicates).

III, IV, and V is found in the ciliate *Nyctotherus* and the stramenopile *Blastocystis* (Müller et al. 2012). In its bloodstream stage, the kinetoplastid *Trypanosoma brucei* shuts down its respiratory chain, activates glycerol-3-phosphate dehydrogenase and an AOX, and to generate proton gradient switches its complex V into the reverse (Tielens and van Hellemond 2009). A "petite" mutant of *T. brucei* termed *T. b. evansi* lost all complexes containing the mitochondrial-encoded subunits except for complex V, where mutations in the nuclear-encoded subunits and an ATP/ADP transporter compensate for the loss of its mitochondrial-encoded subunit atp6 (Dean et al. 2013). Last but not least, numerous anaerobic (e.g., *Entamoeba*, *Giardia*, *Mikrocytos*, and *Trichomonas)* and facultative anaerobic parasitic protists (e.g., *Cryptosporidium* and microsporidia) retained mitochondrion-derived hydrogenosomes and mitosomes, from which the respiratory chain has been lost altogether (Müller et al. 2012; Burki et al. 2013).

It should be noted that, except for *Chromera*, complex III is always lost along with complex IV. Moreover, reductions of the respiratory chain occur almost exclusively in anaerobic organisms, of which the most studied are parasites, yet *Chromera* is a fully aerobic, free-living phototroph, which can live in a simple inorganic medium just in the presence of light (Moore et al. 2008; Oborník et al. 2009). Using a selective inhibitor of complex III, we provide experimental evidence that this complex is indeed absent from *Chromera* but active in *Vitrella*. Moreover, because the SHAM treatment had no effect on the oxygen consumption of *Chromera*, the AOX is, in agreement with our hypothesis, disconnected from the respiratory function. However, the inhibitory effect of a long exposure to SHAM may be a consequence of increased production of radical oxygen species, because a blocked AOX cannot function as a sink for electrons generated by complex II, which may consequently cause damage to the mitochondrial membrane.

Although *Chromera* and *Vitrella* grow under aerobic conditions, they also possess an extensive set of enzymes characteristic for anaerobic protists (table 1 and fig. 3): a [FeFe]-hydrogenase with a complete set of three hydrogenase maturases, pyruvate: NADP oxidoreductase, pyruvate-formate lyase, NADH oxidase, acetaldehyde/alcohol dehydrogenase, acetate: succinate CoA-transferase, and acetyl-CoA synthetase (ADP-forming), to name the most prominent ones. These enzymes are absent in nearly all major lineages of the parasitic apicomplexans, with the exception of the mitosome-bearing human parasite *Cryptosporidium*. This suggests that the life history of *Chromera* may include previously unknown periods under anaerobic conditions or, more importantly, that the common ancestor of apicomplexans was substantially more metabolically diverse than are nearly all of its extant descendants. Such versatility of the mitochondrion has recently emerged in the aerobes *Naegleria* and *Chlamydomonas*, which contain a large set of "anaerobic" enzymes (Müller et al. 2012). Dinoflagellates and perkinsids (Danne et al. 2013), and now even more prominently *Chromera* and *Vitrella*, are joining this club. In fact, *Chromera* qualifies as the most trophically versatile protist, capable of phototrophy, aerobic and strictly anaerobic osmotrophy, and maybe even predation (Oborník et al. 2012; Oborník and Lukeš 2013).

When the respiratory chains of *Chromera* and *Vitrella* are seen in an evolutionary context (fig. 8), it is obvious that the evolution of mitochondrial genomes of alveolates is reductive. We suppose that the mitochondrial genome of an ancestral alveolate underwent linearization, and at a later stage was reduced in all myzozoan lineages through massive loss of protein-coding genes and rRNA fragmentation. In *Chromera*, *Vitrella*, and dinoflagellates, the genome has entered a fragmented and scrambled state due to extensive recombination, but in most apicomplexans it retained its composition from monomeric linear molecules. *Chromera* displays a uniquely reduced mitochondrial genome and possesses a respiratory chain interrupted in an unprecedented fashion. Phylogeny of L-and D-lactate cytochrome *c* oxidoreductases likely donating electrons to complex IV shows that these enzymes are very probably eukaryotic in origin. We can see the same pattern in the evolution of most of alternative ubiquinone reductases (NDH2, ETFQO, G3PDH, and G14LDH). One of the two DHODHs and bacterial SQO in *Chromera* and *Vitrella* are the only genes likely of mitochondrial origins among the detected alternative ubiquinone reductases. This is true just for ubiquinone reductases, as there are more examples of potential LGT in Table 1, see boxed cells. This implies that the entire unusual enzymatic

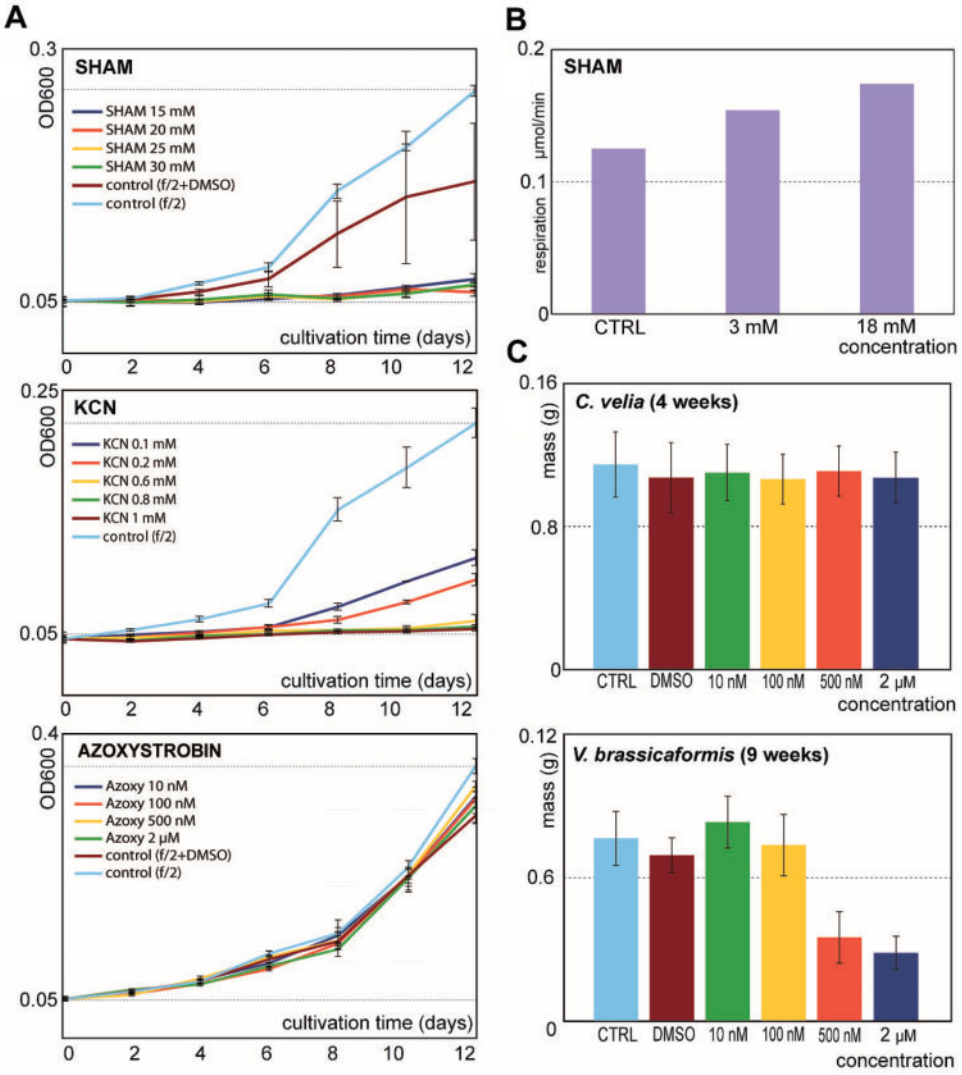

FIG. 7. Growth of *Chromera velia* and *Vitrella brassicaformis* in the presence of specific inhibitors of selected mitochondrial proteins. (A) Growth curves of *Chromera* cultivated in the presence of SHAM, potassium cyanide (KCN), and azoxystrobin. KCN, an inhibitor of cytochrome *c* oxidase (complex IV), slows down the growth. Lack of inhibition by azoxystrobin supports the absence of cytochrome *c* reductase (complex III). (B) SHAM, an inhibitor of AOX, is efficiently inhibiting the growth of *Chromera* at concentrations that did not affect respiration in a short-term treatment. (C) Graphs showing resulting biomass after growth curve experiments. *Chromera* was harvested after reaching the stationary growth phase at 4 weeks. Due to much slower growth, *Vitrella* was harvested after reaching the stationary growth phase at 9 weeks. Biomass for each concentration was calculated as average of five repetitions (standard deviations are shown). High concentration of dimethyl sulfoxide (DMSO) in the media slightly decreases the final biomass.

equipment found in *Chromera* was already present in an ancient eukaryote.

Materials and Methods

The *Chromera* genome was sequenced by combining the following reads (supplementary table S3, Supplementary Material online): single 454 reads (average length ~300 nt), paired-end Illumina MiSeq reads (filtered and trimmed reads <250 nt in length), mate pair Illumina HiSeq reads (filtered and trimmed reads <100 nt in length, insert size 1.7–5.5 kb), and additional paired-end Illumina reads for a fraction enriched for mitochondrial DNA by centrifugation in a CsCl-Hoechst 33258 density gradient (supplementary fig. S14, Supplementary Material online). All the reads were assembled simultaneously using GS De Novo Assembler (Newbler) v.2.9 (see assembly statistics in supplementary table S4, Supplementary Material online), and mitochondrial contigs were identified using BLAST with the apicomplexan cox1, cox3, and cob proteins and rRNA fragments. The Newbler assembler defines contigs as unambiguous parts of a read overlap graph, hence some contigs can be shorter than the reads that make them, with reads flowing from one contig into another (reads can also flow between the ends of long contigs). Therefore, extension of initial gene- or gene fragment-containing contigs was possible by following alternative paths in a graph of direct contig links produced by Newbler (see a detailed example of this approach in supplementary fig. S15, Supplementary Material online). Mitochondrial origin and integrity of the resulting "supercontigs" was verified by mapping on them reads of

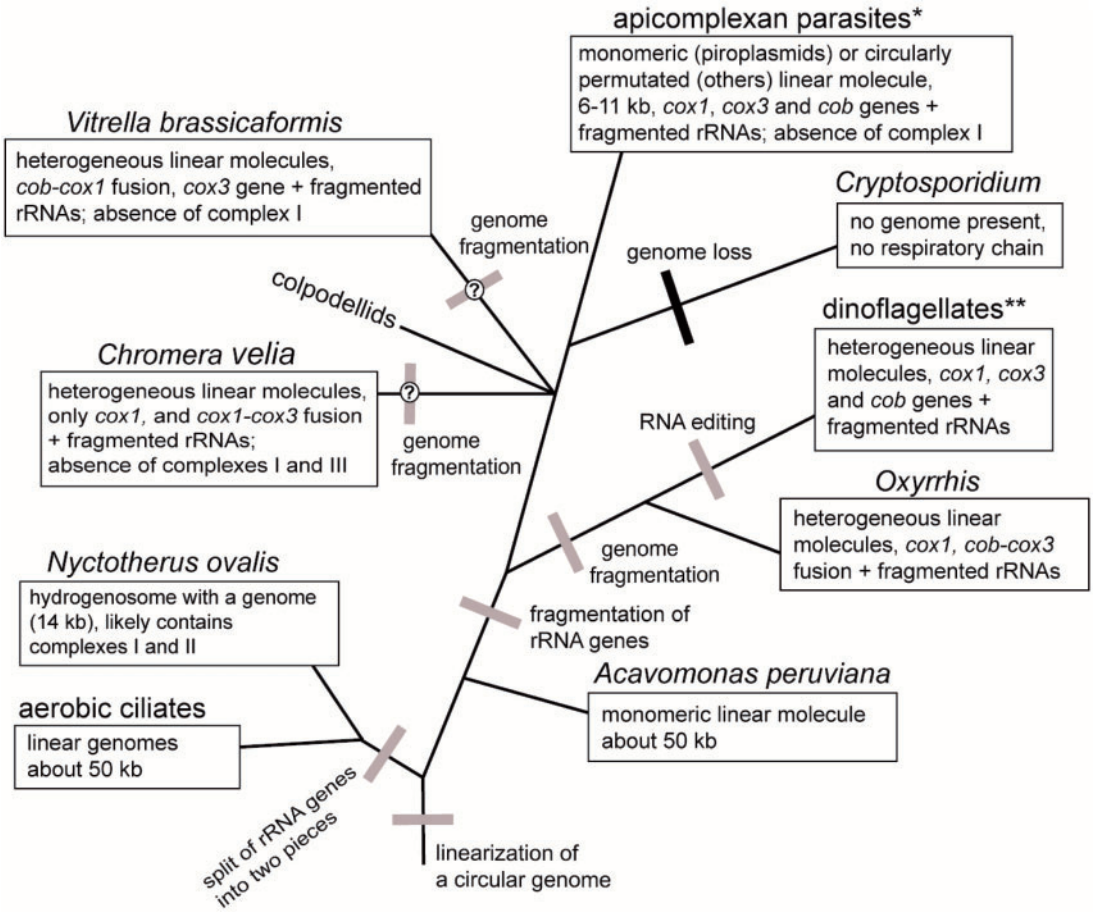

FIG. 8. Overview of the mitochondrial evolution in alveolates.

the mitochondrial DNA-enriched fraction (see an example in supplementary fig. S16, Supplementary Material online) and mate pair reads with long insert size (data not shown), respectively.

The scrambled structure of the *Chromera* mitochondrial genome revealed by 454 and Illumina sequencing was further investigated by PCR and Sanger sequencing (supplementary fig. S17, Supplementary Material online). *Vitrella* mitochondrial contigs were assembled from Illumina HiSeq paired-end and mate pair reads (filtered and trimmed reads <100 nt in length) with Velvet and CLC Genomics Workbench v. 6.5 (see contig sequences in supplementary fig. S5, Supplementary Material online). Transcription of *Chromera* and *Vitrella* mitochondrial contigs was assessed by mapping strand-specific transcriptome reads of poly-A fraction on them (supplementary table S3, Supplementary Material online). The list of transcripts identified in the extended mitochondrial contigs of *Chromera* is shown in supplementary table S2, Supplementary Material online.

Components of the respiratory chain and related enzymes in *Chromera*, *Vitrella*, and in the reference species set (table 1) were identified using at least one HMM per protein, either based on MUSCLE alignments of annotated proteins in alveolates, or taken from the Pfam database or from NCBI CDD. HMM searches were performed with the HMMER3 software using protein-specific *E*-value cutoffs, depending on protein length and the need to distinguish closely related protein families. Sources of HMM models and *E*-value cutoffs for the enzymes most discussed in the paper are shown in table 3. NADH-dependent L-lactate and malate dehydrogenases were distinguished using characteristic residues.

Multiple alignments of cox1, L- and D-lactate: cytochrome *c* oxidoreductases, G14LDH, NADH-dependent D-lactate dehydrogenase, alternative NADH dehydrogenases, ETFQO, glycerol-3-phosphate dehydrogenase, SQO, and DHODH were performed using MUSCLE (Edgar 2004). Alignments were edited, gaps and ambiguously aligned regions were excluded from further analyses. Trees were computed using maximum likelihood (ML) (RAxML; Stamatakis 2014), and Bayesian inference (MrBayes 3.2; Ronquist et al. 2012). ML trees were constructed under the LG model (all proteins except cox1), or cpREV model (cox1), according to ProtTest (Darriba et al. 2011). MrBayes was used to assess Bayesian topologies and PPs using two independent Monte-Carlo Markov chains run under the default settings for 2 million generations. We used 500,000 generations as a burn-in and omitted them from topology reconstruction and PP calculation. Bayesian trees were computed using the Whelan and Goldman model. Putative localizations of enzymes of interest (table 2) were predicted with TargetP (Emanuelsson et al. 2000), SignalP (Petersen et al. 2011), and MitoProt (Claros and Vincens 1996) programs.

Table 3. Sources of HMMs and *E*-Value Cutoffs Used for Identification of Alternative Ubiquinone and Cytochrome *c* Reductases, and Lactate Dehydrogenases with the HMMER3 Software.

Enzyme	Source of HMM: Taxa or Database (accession)	HMM Length, aa	*E*-Value Cutoff
L-Lactate: cytochrome *c* oxidoreductase (cytochrome b_2)	Fungi, *Perkinsus, Karlodinium*	502	10^{-60}
D-Lactate: cytochrome *c* oxidoreductase	NCBI CDD (PLN02805)	563	10^{-160}
Galacto-1,4-lactone: cytochrome *c* oxidoreductase	Pfam (ALO)	260	10^{-50}
NADH-dependent D-Lactate dehydrogenase	NCBI CDD (PRK11183)	567	10^{-50}
NADH-dependent L-lactate dehydrogenase	Apicomplexa[a]	322	10^{-100}
Alternative NADH dehydrogenase	Sarcocystidae	553	10^{-80}
Electron-transfer flavoprotein: ubiquinone oxidoreductase	Pfam (ETF_QO)	110	10^{-30}
Glycerol-3-phosphate dehydrogenase	Aconoidasida	625	10^{-100}
Sulfide: ubiquinone oxidoreductase	Prokaryotes and eukaryotes	418	10^{-30}
Dihydroorotate: ubiquinone oxidoreductase	Apicomplexa	442	$1e^{-80}$

[a]The model for NADH-dependent L-lactate dehydrogenase detects malate dehydrogenase as well, and distinguishing these enzymes requires analysis of characteristic residues in the alignment.

The mitochondrial DNA-enriched sample was prepared for electron microscopy by the cytochrome *c* method (Ferguson and Davis 1978). Plasmid pGEM served as a standard. The samples were examined with a Philips CM12 electron microscope at 80 kV, with precise magnification determined using replica grating.

For making growth curves, Azoxystrobin (Sigma) was dissolved in DMSO (stock solution 10 mg/ml), and a series of five concentrations in the f/2 medium ranging from 10 to 2,000 ng/ml was prepared. Each concentration and negative controls were assayed in three replicates. Cultivation flasks containing 20 ml of medium were inoculated with 0.5 ml of starting culture. Three replicates of *Chromera* culture were observed every other day for 2 weeks by measuring absorbance changes (OD_{600}, fig. 3*A*) three times. For biomass measurements the culture was grown as described above, and after 4 weeks the resulting biomass from equal volume of five replicates was harvested, dried, and weighted (fig. 3*C*). Due to extremely tight clustering in clumps, *Vitrella* is suitable for neither absorbance measurement, nor cell counting. Also, in contrast to *Chromera*, *Vitrella* culture grows much slower. Therefore, only total biomass after 9 weeks was determined (fig. 3*C*).

For measurement of respiration in intact cells, exponentially growing *C. velia* culture was harvested by centrifugation, and cells were washed and resuspended in the f/2 medium at a concentration of approximately 3×10^8 cells/ml. Oxygen consumption at 26 °C was determined using a Clarktype electrode (Theta 90, Czech Republic) in the dark. After 4 min stabilization, SHAM was added to final concentrations of 3 and 18 mM (fig. 7*B*). Cells were incubated for 2–4 min with each concentration of the drug and O_2 consumption was then converted to micromol/min. Respiration with no inhibitors was taken as 100%.

Sequences reported in this article have been deposited in the NCBI BioProject (Accession No. PRJEB6670, PRJEB667) database, in Short Read Archive (Accession No. ERR558149, ERR558150, ERR558151, ERR558152, ERR558194, ERR558195 , ERR558196, ERR558197, ERR558198, ERR558199, ERR558200, ERR558201, ERR558202, ERR571482, ERR571483, ERR571484, ERR571485), and in NCBI Genbank (see supplementary table S1, Supplementary Material online). The annotated nuclear genomes of *C. velia* and *V. brassicaformis* have been deposited in EuPathDB (eupathdb.org).

Acknowledgments

The authors thank the KAUST Bioscience Core Laboratory personnel for sequencing Illumina libraries used in this project, Evgeny S. Gerasimov (Institute for Information Transmission Problems, Russian Academy of Sciences, Moscow) and Martin Kolísko (University of British Columbia, Vancouver) for help with sequence analysis, Oldřich Benada (Institute of Microbiology, Prague) for help with electron microscopy, Anton Horváth (Comenius University, Bratislava), Dave Speijer (University of Amsterdam, Amsterdam), and Ivan Hrdý (Charles University, Prague) for useful comments. This work was supported by Czech Science Foundation grants P506/12/1522, 13-33039S (support for J.M.) and P501/12/G055 (support for A.T.) to M.O., project Algatech (CZ.1.05/2.1.00/03.0110) to M.O., FP7 agreement 316304 to M.O. and J.L., the KAUST award FIC/2010/09 to A.P., M.O. and J.L., and by a grant from the Canadian Institutes for Health Research to P.J.K. and J.L. is also supported by the Praemium Academiae, and P.F. by a grant of the Moravian-Silesian region (project MSK2013-DT1) and by Russian Foundation for Basic Research (project 14-04-31936). P.J.K. and J.L. are Senior Fellows and J.J. is a Global Scholar at the Canadian Institute for Advanced Research, and P.J.K. was supported by a Fellowship from the John Simon Guggenheim Foundation.

References

Akhmanova A, Voncken F, van Alen T, van Hock A, Boxma B, Vogels G, Veenhuist M, Hackstein JHP. 1998. A hydrogenosome with a genome. *Nature* 396:527–528.

Balba H. 2007. Review of strobilurin fungicide chemicals. *J Environ Sci Health. B* 42:441–451.

Burger G, Gray MW, Forget L, Lang BF. 2013. Strikingly bacteria-like and gene-rich mitochondrial genomes throughout jakobid protists. *Genome Biol Evol.* 5:418–438.

Burger G, Gray MW, Lang BF. 2003. Mitochondrial genomes: anything goes. *Trends Genet.* 12:709–716.

Burki F, Corradi N, Sierra R, Pawlowski J, Meyer GR, Abbott CL, Keeling PJ. 2013. Phylogenomics of the intracellular parasite *Mikrocytos mackini* reveals evidence for a mitosome in rhizaria. *Curr Biol.* 23: 1541–1547.

Burki F, Flegontov P, Oborník M, Cihlář J, Pain A, Lukeš J, Keeling PJ. 2012. Re-evaluating the green versus red signal in eukaryotes with secondary plastid of red algal origin. *Genome Biol Evol.* 4: 626–635.

Claros MG, Vincens P. 1996. Computational method to predict mitochondrially imported proteins and their targeting sequences. *Eur J Biochem.* 241:779–786.

Danne JC, Gornik SG, Macrae JI, McConville MJ, Waller RF. 2013. Alveolate mitochondrial metabolic evolution: dinoflagellates force reassessment of the role of parasitism as a driver of change in apicomplexans. *Mol Biol Evol.* 30:123–139.

Darriba D, Taboada GL, Doallo R, Posada D. 2011. ProtTest 3: fast selection of best-fit models of protein evolution. *Bioinformatics* 27: 1164–1165.

Dean S, Gould MK, Dewar CE, Schnaufer AC. 2013. Single point mutations in ATP synthase compensate for mitochondrial genome loss in trypanosomes. *Proc Natl Acad Sci U S A.* 110:14741–14746.

Edgar RC. 2004. MUSCLE: multiple sequence alignment with high accuracy and high throughput. *Nucleic Acids Res.* 32:1792–1797.

Emanuelsson O, Nielsen H, Brunak S, von Heijne G. 2000. Predicting subcellular localization of proteins based on their N-terminal amino acid sequence. *J Mol Biol.* 300:1005–1016.

Feagin JE, Mericle BL, Werner E, Morris M. 1997. Identification of additional components of the fragmented rRNAs of the two *Plasmodium falciparum* 6 kb element. *Nucleic Acids Res.* 25:438–446.

Ferguson J, Davis RW. 1978. A new electron microscopic technique for establishing the positions of genes: an analysis of the yeast ribosomal RNA coding region. *J Mol Biol.* 123:417–430.

Ginger ML, Fritz-Laylin LK, Fulton C, Cande WZ, Dawson SC. 2010. Intermediary metabolism in protists: a sequence-based view of facultative anaerobic metabolism in evolutionarily diverse eukaryotes. *Protist* 161:642–671.

Gray MW, Lang BF, Burger G. 2004. Mitochondria of protists. *Annu Rev Genet.* 38:477–524.

Gray MW, Lukeš J, Archibald JM, Keeling PJ, Doolittle WF. 2010. Cell biology. Irremediable complexity? *Science* 330:920–921.

Imanian B, Keeling PJ. 2007. The dinoflagellates *Durinskia baltica* and *Kryptoperidinium foliaceum* retain functionally overlapping mitochondria from two evolutionarily distinct lineages. *BMC Evol Biol.* 7:172.

Jackson CJ, Norman JE, Schnare MN, Gray MW, Keeling PJ, Waller RF. 2007. Broad genomic and transcriptional analysis reveals a highly derived genome in dinoflagellate mitochondria. *BMC Biol.* 5:41.

Janouškovec J, Horák A, Oborník M, Lukeš J, Keeling PJ. 2010. A common red algal origin of the apicomplexan, dinoflagellate, and heterokont plastids. *Proc Natl Acad Sci U S A.* 107:10949–10954.

Janouškovec J, Sobotka R, Lai DH, Flegontov P, Koník P, Komenda J, Ali S, Prášil O, Pain A, Oborník M, et al. 2013. Split photosystem protein, linear-mapping topology, and growth of structural complexity in the plastid genome of *Chromera velia*. *Mol Biol Evol.* 30: 2447–2462.

Janouškovec J, Tikhonenkov DV, Mikhailov KV, Simdyanov TG, Aleoshin VV, Mylnikov AP, Keeling PJ. 2013. Colponemids represent multiple ancient alveolate lineages. *Curr Biol.* 23:2546–2552.

Kamikawa R, Inagaki Y, Sako Y. 2007. Fragmentaton of mitochondrial large subunit rRNA in the dinoflagellate Alexandrium catenella and the evolution of rRNA structure in alveolate mitochondria. *Protist* 158:239–245.

Kamikawa R, Nishimura H, Sako Y. 2009. Analysis of the mitochondrial genome, transcripts, and electron transport activity in the dinoflagellate *Alexandrium catenella* (Gonyaulacales, Dinophyceae). *Phycol Res.* 57:1–11.

Lukeš J, Hashimi H, Zíková A. 2005. Unexplained complexity of the mitochondrial genome and transcriptome in kinetoplastid flagellates. *Curr Genet.* 48:277–299.

Marcet-Houben M, Marceddu G, Gabaldon T. 2009. Phylogenomics of the oxidative phosphorylation in fungi reveals extensive gene duplication followed by functional divergence. *BMC Evol Biol.* 9:295.

Masuda I, Matsuzaki M, Kita K. 2010. Extensive frameshift at all AGG and CCC codons in the mitochondrial cytochrome c oxidase subunit 1 gene of *Perkinsus marinus* (Alveolata; Dinoflagellata). *Nucleic Acids Res.* 38:6186–6194.

Moore RB, Oborník M, Janouškovec J, Chrudimský T, Vancová M, Green DH, Wright SW, Davies NW, Bolch CJ, Heimann K, et al. 2008. A photosynthetic alveolate closely related to apicomplexan parasites. *Nature* 451:959–963.

Müller M, Mentel M, van Hellemond JJ, Henze K, Woehle C, Gould SB, Yu RY, van der Giezen M, Tielens AG, Martin WF. 2012. Biochemistry and evolution of anaerobic energy metabolism in eukaryotes. *Microbiol Mol Biol Rev.* 76:444–495.

Nash EA, Barbrook AC, Edwards-Stuart RK, Bernhardt K, Howe CJ, Nisbet ER. 2007. Organization of the mitochondrial genome in the dinoflagellate *Amphidinium carterae*. *Mol Biol Evol.* 24:1528–1536.

Nash EA, Nisbet RER, Barbrook AC, Howe CJ. 2008. Dinoflagellates: a mitochondrial genome all at sea. *Trends Genet.* 24:328–335.

Oborník M, Janouškovec J, Chrudimský T, Lukeš J. 2009. Evolution of the apicoplast and its hosts: from heterotrophy to autotrophy and back again. *Int J Parasitol.* 39:1–12.

Oborník M, Lukeš J. 2013. Cell biology of chromerids: autotrophic relatives to apicomplexan parasites. *Int Rev Cell Mol Biol.* 306:333–369.

Oborník M, Modrý D, Lukeš M, Černotíková-Stříbrná E, Cihlář J, Tesařová M, Kotabová E, Vancová M, Prášil O, Lukeš J. 2012. Morphology, ultrastructure and life cycle of *Vitrella brassicaformis* n. sp., n. gen., a novel chromerid from the Great Barrier Reef. *Protist* 163:306–323.

Petersen J, Ludewig AK, Michael V, Bunk B, Jarek M, Baurain D, Brinkmann H. 2014. *Chromera velia*, endosymbioses and the rhodoplex hypothesis-plastid evolution in cryptophytes, alveolates, stramenopiles, and haptophytes (CASH lineages). *Genome Biol Evol.* 6: 666–684.

Petersen TN, Brunak S, von Heijne G, Nielsen H. 2011. SignalP 4.0: discriminating signal peptides from transmembrane regions. *Nat Methods.* 8:785–786.

Porcel BM, Denoeud F, Opperdoes F, Noel B, Madoui MA, Hammarton TC, Field MC, Da Silva C, Couloux A, Poulain J, et al. 2014. The streamlined genome of *Phytomonas* spp. relative to human pathogenic kinetoplastids reveals a parasite tailored for plants. *PLoS Genet.* 10:e100400.

Ronquist F, Teslenko M, van der Mark P, Ayres DL, Darling A, Höhna S, Larget B, Liu L, Suchard MA, Huelsenbeck JP. 2012. MrBayes 3.2: efficient Bayesian phylogenetic inference and model choice across a large model space. *Syst Biol.* 61:539–542.

Sheiner L, Vaidya AB, McFadden GI. 2013. The metabolic roles of the endosymbiotic organelles of *Toxoplasm*a and *Plasmodium* spp. *Curr Opin Microbiol.* 16:452–458.

Slamovits CH, Saldarriaga JF, Larocque A, Keeling PJ. 2007. The highly reduced and fragmented mitochondrial genome of the early-branching dinoflagellate *Oxyrrhis marina* shares characteristics with both apicomplexan and dinoflagellate mitochondrial genomes. *J Mol Biol.* 372:356–368.

Stamatakis A. 2014. RAxML version 8: a tool for phylogenetic analysis and post-analysis of large phylogenies. *Bioinformatics* 30:1312–1313.

Tielens AG, van Hellemond JJ. 2009. Surprising variety in energy metabolism within Trypanosomatidae. *Trends Parasitol.* 25: 482–490.

Tikhonenkov DV, Janouškovec J, Mylnikov AP, Mikhailov KV, Simdyanov G, Aleoshin VV, Keeling PJ. 2014. Description of *Colponema vietnamica* sp.n. and *Acavomonas peruviana* n. gen. n. sp., two new alveolate phyla (Colponemidia nom. nov. and Acavomonidia nom. nov.) and their contributions to reconstructing the ancestral state of alveolates and eukaryotes. *PLoS One* 9:e95467.

Vaidya AB, Mather MW. 2009. Mitochondrial evolution and functions in malaria parasites. *Annu Rev Microbiol.* 63:249–267.

van Dooren GG, Stimmler LH, McFadden GI. 2006. Metabolic maps and functions of the Plasmodium mitochondrion. *FEMS Microbiol Rev.* 30:596–630.

Waller RF, Jackson CJ. 2009. Dinoflagellate mitochondrial genomes: stretching the rules of molecular biology. *Bioessays* 31:237–245.

Waller RF, Keeling PJ. 2006. Alveolate and chlorophycean mitochondrial *cox2* genes split twice independently. *Gene* 383:33–37.

Woehle C, Dagan T, Martin WF, Gould SB. 2011. Red and problematic green phylogenetic signals among thousands of nuclear genes from the photosynthetic and apicomplexa-related *Chromera velia*. *Genome Biol Evol.* 3:1220–1230.

Yurchenko V, Hobza R, Benada O, Lukeš J. 1999. *Trypanosoma avium*: large minicircles in the kinetoplast DNA. *Exp Parasitol.* 92: 215–218.

Zhang H, Campbell DA, Sturm NR, Dungan CF, Lin S. 2011. Spliced leader RNAs, mitochondrial gene frameshifts and multi-protein phylogeny expand support for the genus *Perkinsus* as a unique group of alveolates. *PLoS One* 6:e19933.